JACS
JOURNAL OF THE AMERICAN CHEMICAL SOCIETY
Article
pubs.acs.org/JACS

Fluorescence Enhancement of Di-*p*-tolyl Viologen by Complexation in Cucurbit[7]uril

Marina Freitag, Lars Gundlach,† Piotr Piotrowiak, and Elena Galoppini*

Chemistry Department, Rutgers University, 73 Warren Street, Newark, New Jersey 07102, United States

Supporting Information

ABSTRACT: A viologen derivative, 1,1′-di-*p*-tolyl-(4,4′-bipyridine)-1,1′-diium dichloride (DTV^{2+}), was studied in solution and encapsulated in cucurbit[7]uril (CB7), a macrocyclic host. Upon encapsulation, DTV^{2+} exhibited dramatically enhanced fluorescence. Aqueous solutions of DTV^{2+} were weakly fluorescent (Φ = 0.01, τ < 20 ps), whereas the emission of the DTV^{2+}@2CB7 complex was enhanced by 1 order of magnitude (Φ = 0.12, τ = 0.7 ns) and blue-shifted by 35 nm. Similar properties were observed in the presence of NaCl. DTV^{2+} in a poly(methyl methacrylate) matrix was fluorescent with a spectrum similar to that observed for the complex in solution. ^{1}H NMR and UV−vis titrations indicated that the DTV^{2+}@2CB7 complex is formed in aqueous solutions with complexation constants $K_1 = (1.2 \pm 0.3) \times 10^4$ M^{-1} and $K_2 = (1.0 \pm 0.4) \times 10^4$ M^{-1} in water. Density functional theory and configuration interaction singles calculations suggested that the hindrance of the rotational relaxation of the S_1 state of DTV^{2+} caused by encapsulation within the host or a polymer matrix plays a key role in the observed emission enhancement. The absorption and emission spectra of DTV^{2+}@2CB7 in water exhibited a large Stokes shift (ΔSt ~ 9000 cm^{-1}) and no fine structure. DTV^{2+} is a good electron acceptor [$E°(DTV^{2+}/DTV^{\bullet+})$ = −0.30 V vs Ag/AgCl] and a strong photooxidant [$E°(DTV^{*2+}/DTV^{\bullet+})$ = 0.09 V vs NHE]).

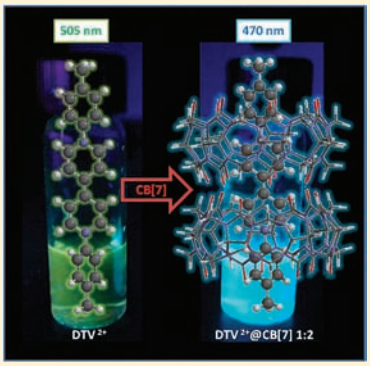

INTRODUCTION

Viologens (1,1′-disubstituted-4,4′-bipyridinium salts)[1] have wide-ranging applications including electrochromic displays,[2−5] molecular electronics,[6,7] and redox sensors[8,9] and are used in the design of cyclophane,[10−13] rotaxane,[14−16] and catenane[17−19] molecular hosts. They are common herbicides because of their phytotoxicity and bind strongly to DNA.[20] Viologens are excellent electron acceptors and, in a fast and reversible redox process, form a radical cation that is stable and intensely colored.[1,2] Because of these properties, viologens are widely used as acceptors in electron-transfer studies[21−23] and as components of novel electrochromics.[2−4] Also, they have been employed as redox mediators in photocatalytic hydrogen production[24−26] as well as in enzymatic activity studies.[27,28]

Methyl viologen (1,1′-dimethyl-4,4′-bipyridine-1,1′-diium, MV^{2+}) dichloride forms a stable complex with cucurbit[7]uril (CB7), a water-soluble macrocyclic host consisting of seven glycoluril units that has a portal diameter of 5.4 Å, an inner diameter of 7.3 Å, and a high affinity for positively charged compounds (Figure 1).[29−31] The host−guest chemistry, the complexation constant (K_c ~ 10^5 M^{-1}), and the redox properties of the MV^{2+}@CB7 complex have been extensively investigated.[32−34] More recently, we reported the electrochromic properties of CB7 complexes of MV^{2+} and 1-methyl-1′-*p*-tolyl-4,4′-bipyridine-1,1′-diium (MTV^{2+}) physisorbed on nanoparticle TiO_2 thin films.[35]

While the redox chemistry of viologen is well-characterized, the excited-state deactivation mechanism of photoexcited viologen in fluid solutions has been the object of debate in the past.[36−38] It has frequently been reported that methyl viologen does not fluoresce in solution.[39−42] Reports of fluorescence are controversial, partly because highly fluorescent pyridone impurities may be present in viologen samples.[43] Fluorescence was reported for MV^{2+} embedded in zeolites[44] and for 2,7-dimethylthieno(2,3-*c*:5,4-*c*′)dipyridinium,[45] a methyl viologen with a thienyl bridge locking the pyridinium rings in a rigid planar structure. The fluorescence and excited-state properties of MV^{2+} were thoroughly characterized for the first time a decade ago by Kohler and co-workers.[46] The dynamics of the S_1 excited state was found to be strongly dependent on the solvent, with a fluorescence quantum yield (Φ) of ~0.03 and a decay lifetime (τ) of ~1 ns in acetonitrile, in contrast with a decay lifetime of several picoseconds in water and even faster decay in methanol. In water, the fast excited-state decay was ascribed to a nonradiative channel. In methanol, quenching of the S_1 excited state of MV^{2+} involves electron transfer from the solvent.[46]

This paper describes an unprecedented fluorescence enhancement observed in aqueous solutions of complexes formed by CB7 and 1,1′-di-*p*-tolyl-4,4′-bipyridine-1,1′-diium (DTV^{2+}, **1**) dichloride (Figure 1). The viologen DTV^{2+}, which carries two *p*-tolyl groups on the quaternized nitrogens, was synthesized as part of our interest in the electrochromic properties of viologen@CB7 complexes bound to TiO_2.[35] We noticed that solutions of DTV^{2+} were weakly fluorescent and

Received: July 21, 2011
Published: February 9, 2012

   dx.doi.org/10.1021/ja206833z | *J. Am. Chem. Soc.* 2012, 134, 3358−3366

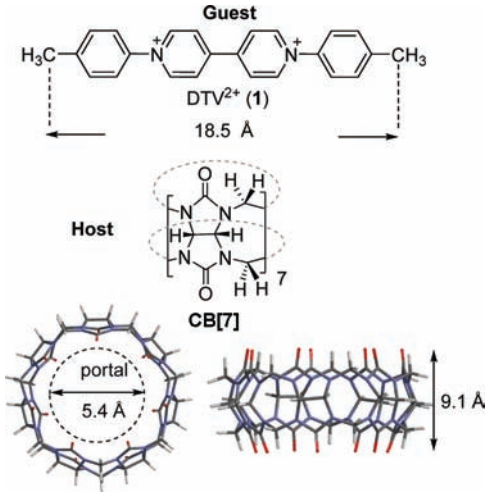

Figure 1. (top) Molecular structure of DTV^{2+}, the viologen derivative studied in this work. The counterion is chloride. (bottom) Molecular structure and dimensions of CB7. The structures of CB7 (top and side view) are not in scale.

that encapsulation in CB7 produced a strong blue emission. Similar behavior was observed for MTV^{2+},[35] a viologen with one methyl group and one *p*-tolyl group on the quaternized nitrogens, while no fluorescence emission enhancement upon encapsulation in CB7 was observed for MV^{2+} or phenyl viologen. First, the possibility that this effect was due to an emissive impurity had to be ruled out. Although the presence of traces of impurities could not be excluded completely, comparisons of different batches of DTV^{2+} after repeated purification steps, combined with quantum yield and emission lifetime studies, elemental analysis, and titration experiments with CB7, confirmed that the observed fluorescence enhancement reported here is caused by encapsulation of DTV^{2+}.

The emissive properties of DTV^{2+}@CB7 are interesting for a number of reasons. To the best of our knowledge, this is the first example of fluorescence enhancement of a viologen derivative induced by encapsulation in a molecular host. In one of the first studies of fluorophore@CB7 complexes, Nau and co-workers reported that encapsulation of 2,3-diazabicyclo[2.2.2]oct-2-ene (DBO) in CB7 resulted in a 2-fold increase in emission lifetime caused by the host shielding the guest from quenchers (e.g., oxygen).[47] More recently, emission enhancement of complexes of CBs with a variety of fluorescent dyes has attracted considerable attention for potential applications as fluorescent probes for biological systems,[48] in fluorescence lifetime imaging microscopy (FLIM),[49] as water-soluble sensors,[34] and in supramolecular photochemistry studies.[47,50,51] The ability to extend this type of host–guest photochemistry to viologens is an important development, especially because we previously demonstrated that CB7 and its viologen complexes bind to nanostructured metal oxide films that were used to prepare fully reversible electrochromic windows.[35] Hybrid organic/inorganic layers prepared from emissive CB7 complexes can extend the possible applications to light-emitting diodes. The advantages of the host–guest chemistry (inhibited quenching, chemical stability, etc.) are important for fundamental charge-transfer studies at semiconductor interfaces.[52]

The fact that DTV^{2+} exhibited enhanced fluorescence in CB7 while methyl viologen and the structurally similar phenyl viologen did not is intriguing. While the host–guest chemistry of alkyl viologen@CB7 complexes has been extensively investigated,[31−35] fluorescence has never been reported. This suggests that the *p*-tolyl group is important for the observed fluorescence enhancement. The reason for the observed fluorescence enhancement and the influence of the *p*-tolyl group are the main focus of this work.

In this work, we studied the complexation of DTV^{2+} in CB7 in aqueous solutions to determine the complexation constants, the stoichiometry of the complex, the electrochemical properties, and the steady-state and time-resolved fluorescence properties of DTV^{2+} and its complexes with CB7. The experiments were complemented with density functional theory (DFT) and configuration interaction singles (CIS) calculations of the S_1 and T_1 excited states of DTV^{2+}. In addition, we investigated the effect of excess NaCl on the complexation of DTV^{2+} in CB7 and the resulting emission. Cucurbiturils have multiple carbonyl binding sites for positive ions and tend to complex strongly with salts,[53,54] especially NaCl, for which the complexation constant is ∼120 M^{-1}.[55,56] The presence of salts influences the complexation equilibria and, in some cases, the emissive properties of the chromophoric guests.[57,58]

EXPERIMENTAL SECTION

^{1}H NMR Titration in Figure 2. Stock solutions of DTV^{2+} (1 mM) and CB7 (2 mM) were prepared in D_2O. The stock solutions were combined in an NMR tube to obtain the desired host:guest ratio. The same experiment was repeated in the presence of 50 mM NaCl.

Electrochemistry. Cyclic voltammograms were collected on a BAS CV27 potentiostat. The measurements were conducted on 0.5 mM DTV^{2+} aqueous solutions with 0.1 M phosphate buffer (pH 7.3), following literature methods.[33] The solutions were deaerated before and during the measurements by bubbling nitrogen in a standard three-electrode arrangement with a glassy carbon electrode (2 mm diameter), a Pt gauze auxiliary electrode, and a Ag/AgCl(3.0 M NaCl) reference electrode. The scan rate was 100 mV/s at a sensitivity of 100 mA/V between −0.1 and −0.5 V. All values are reported in volts versus Ag/AgCl.

Spectroscopic Measurements. UV–vis absorbance spectra were collected at room temperature on a Varian Cary 500 spectrophotometer.

Steady-state fluorescence spectra were acquired and recorded at room temperature on a Varian Cary Eclipse fluorescence spectrophotometer calibrated with a standard NIST tungsten halogen lamp.

Fluorescence quantum yields (Φ) were calculated using eq 1:

$$\Phi_{sample} = \Phi_{ref}\left(\frac{A_{ref}}{A_{sample}}\right)\left(\frac{I_{sample}}{I_{ref}}\right)\left(\frac{\eta^2_{sample}}{\eta^2_{ref}}\right) \quad (1)$$

where A_{sample} and A_{ref} are the absorbances at λ_{ex} = 320 nm for the sample and reference, η_{sample} and η_{ref} are the refractive indexes of the solvent used for the sample and reference solutions, and I_{sample} and I_{ref} are the integrated emission intensities of the sample and reference, respectively. Stilbene 420 (2,2″-([1,1′-biphenyl]-4,4′-diyldi-2,1-ethenediyl)bisbenzenesulfonic acid disodium salt) in ethanol was used as the reference (Φ_{ref} = 0.52 in water and 0.80 in 9:1 ethanol/water),[59] with integration over the 375–600 range. No significant changes in the emission quantum yield or fluorescence lifetime measurements were observed in deaerated solutions (freeze–pump–thaw) or in the presence of air, so all of the reported spectra were collected in the presence of air.

Time-resolved fluorescence measurements were collected after excitation with 320 nm, ∼30 fs pulses (∼2 nJ) from a Ti:sapphire-pumped non-collinear optical parametric amplifier. Picosecond time-resolved measurements were performed in a 10 mm cuvette. The fluorescence was collected via a lens and focused onto a Hamamatsu H5783-01 photomultiplier. For some of the measurements, a 500 nm

dx.doi.org/10.1021/ja206833z | J. Am. Chem. Soc. 2012, 134, 3358–3366

band-pass filter was employed (40 nm fwhm). The signal was recorded with a Becker & Hickl PCS 150 sampling card and a PC (50 s sampling time). Femtosecond time-resolved measurements were performed in a 1 mm cuvette. The fluorescence was detected in a Kerr-gated fluorescence spectrometer.[60]

The titration experiments shown in Figures 4b and 5a were conducted by recording the integrated emission spectra of DTV^{2+} (2 mL of a 5 μM aqueous solution) upon addition of 20 μL aliquots of a 100 μM CB7 solution in water.

Preparation of DTV^{2+} in PMMA Polymer Matrix Films. Polymer coatings were prepared by dissolving poly(methyl methacrylate) (PMMA) in formic acid (10 wt %) and adding DTV^{2+} (0.8 wt %) to the solution. Formic acid was a good spin-coating solvent for both PMMA and DTV^{2+}. A SCS|G3P-8 Spin-Coat System (Specialty Coating Systems, Inc.) was used to prepare thin films on a 1 cm × 1 cm cleaned glass slide at 2000 rpm. The resulting PMMA films contained ~8 wt % DTV^{2+}.

DFT and CIS calculations. Geometry optimization and spectral calculations were done using the Spartan'10 software package (Wavefunction, Inc.). The DFT geometry optimizations of the S_0 ground state and the T_1 triplet state of the dication were performed using the B3LYP pseudopotential and a 31-G* basis set. Optimization of the S_1 state and the calculation of the S_0–S_1 transition energies at the equilibrium geometries of the S_0 and S_1 states were performed at the CIS level utilizing the same 31-G* basis set.

RESULTS AND DISCUSSION

Synthesis. There is one report in the literature of DTV^{2+}(**1**),[61] but the synthesis and properties of **1** have not been reported. DTV^{2+} was synthesized in 30% yield in two steps from 4,4′-bipyridine (**2**) using the Zincke reaction,[62] which converts pyridines into pyridinium salts (Zincke salts) by the reaction of 2,4-dinitrochlorobenzene (**3**) and an aniline derivative (Scheme 1; also see the Supporting Information).[63] 1,1′-Bis(2,4-dinitrophenyl)-(4,4′-bipyridine)-1,1′-diium chloride (**4**) was obtained in 44% yield by reaction of **3** with **2**. Reaction of *p*-toluidine (**5**) with **4** yielded the dichloride salt of **1** in 90% yield. DTV^{2+}, a very pale yellow powder, is soluble in protic, polar solvents such as water, ethanol, and methanol.

^{1}H NMR Study of the Complexation of DTV^{2+} with CB7. The formation of DTV^{2+}@CB7 host–guest complexes was monitored by ^{1}H NMR titrations in D_2O (Figure 2, top). The complexation in CB7 resulted in significant encapsulation-induced chemical shifts of the viologen guest protons.[33] The same experiment was repeated in the presence of a large excess of sodium chloride (0.05 M NaCl) (Figure 2, middle).

Upon addition of 0.5 equiv of CB7, the tolyl group's doublets (H_c and H_b) broadened considerably, and all of the signals assigned to the tolyl group (H_a, H_b, and H_c) exhibited a considerable upfield shift (Figure 2, top). The $\Delta\delta$ pattern suggests that CB7 preferentially encapsulates the *p*-tolyl moiety (Figure 2, bottom). We made a similar observation with MTV^{2+},[35] and this might be explained by the propensity of the hydrophobic inner cavity of CB7 to accommodate the hydrophobic tolyl unit in an aqueous environment.

A remarkable broadening of the 4,4′-bipyridyl proton signals at the initial stages of the titration with CB7 were observed. A similar broadening of the ^{1}H NMR spectra for CB7 complexes of viologens has been reported previously by Kaifer and co-workers.[64–66] A plausible explanation for this behavior is that when the guest is in excess, there is a dynamic distribution of species during the time scale of the NMR experiment. Such equilibria could include shuttling of the host along the backbone of DTV^{2+}, partial threading, or a complexation/decomplexation process.

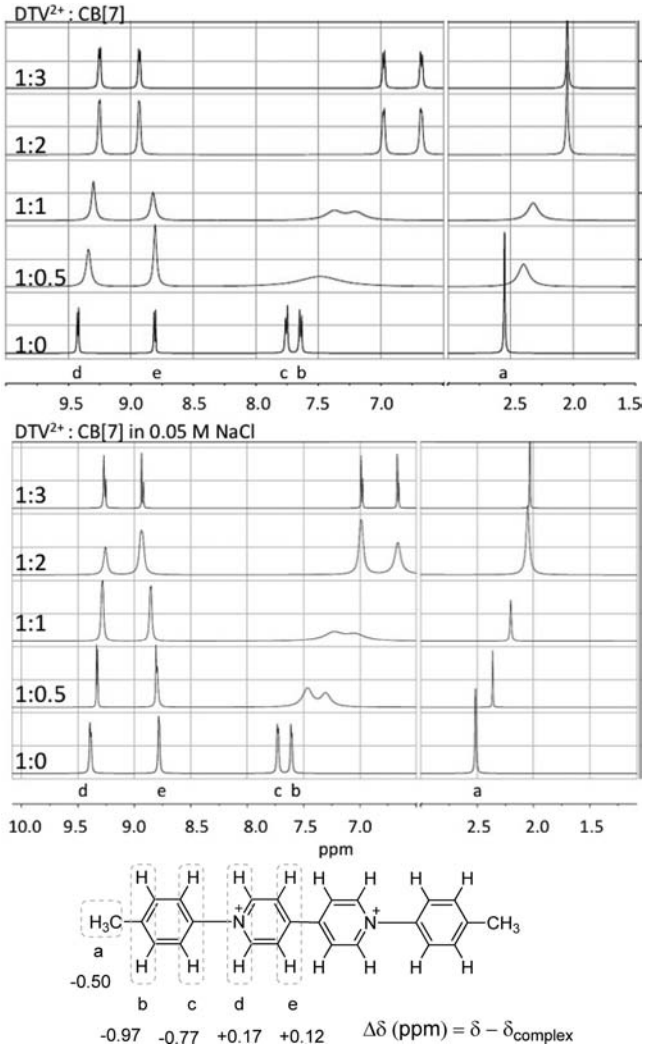

Figure 2. (top) Viologen region of the ^{1}H NMR spectra (in D_2O) of DTV^{2+} alone and after addition of 0.5, 1.0, 2.0, and 3.0 equiv of CB7. The 3–6 ppm region and the CB7 and solvent signals have been omitted for clarity. (middle) Viologen region of the ^{1}H NMR spectra (in 0.05 M NaCl in D_2O) of DTV^{2+} alone and after addition of 0.5, 1.0, 2.0, and 3.0 equiv of CB7. (bottom) Chemical shift differences for DTV^{2+} upon complexation with 2 equiv of CB7 in D_2O. Similar shifts were observed in the presence of NaCl.

The spectrum of the 1:2 guest:host (G:H) ratio was sharper, with the protons of the *p*-tolyl groups exhibiting the largest shifts ($\Delta\delta_{H_b}$ = −0.97 ppm, $\Delta\delta_{H_c}$ = −0.77 ppm, and $\Delta\delta_{H_a}$ = −0.50 ppm) and the 4,4′-bipyridyl protons H_d and H_e exhibiting shifts that are typically observed upon encapsulation of viologens in CB7 (Figure 2).[33] Additional amounts of CB7 did not result in significant spectral changes, indicative of the complete encapsulation of DTV^{2+}, starting from the 1:2 G:H ratio. The spectral changes in the CB7 region (shown in Figure S3 in the Supporting Information) also suggested a 1:2 G:H complex, as the symmetry of the two rims of each CB7 host was disrupted. In the presence of a large excess of NaCl, the spectrum of free DTV^{2+} was unchanged (Figure 2, middle). Upon addition of CB7, the proton signals broadened and became sharp at a G:H ratio of 1:3, suggesting that binding is weaker in the presence of NaCl. In summary, the ^{1}H NMR spectral evolution during titration with increasing amounts of host indicates that a dynamic distribution of various complex

dx.doi.org/10.1021/ja206833z | J. Am. Chem. Soc. 2012, 134, 3358–3366

Scheme 1. Synthesis of DTV^{2+}

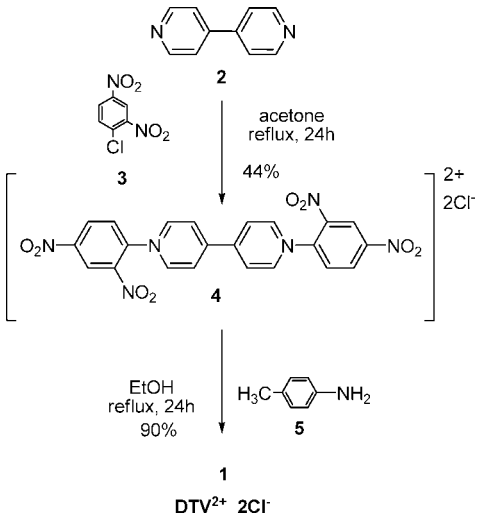

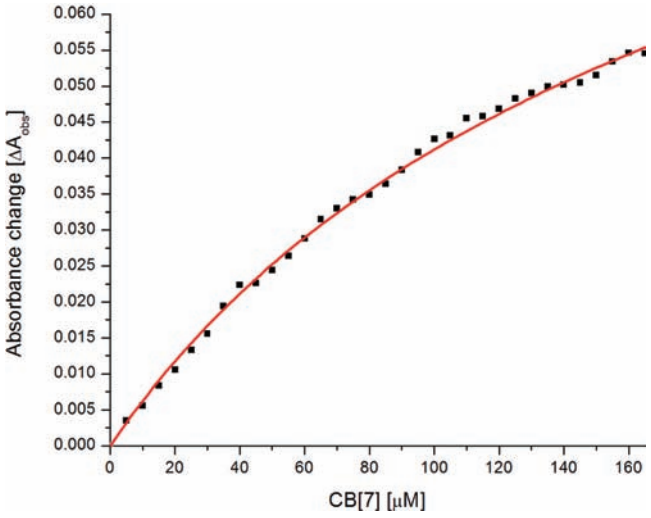

Figure 3. Experimental absorbance changes (ΔA_{obs}) at λ = 335 nm (■) and the fit to eq 4 (red solid line) in the titration of 5 μM DTV^{2+} with CB7 in water.

species is observed when the host is in substoichiometric amount and that full encapsulation of DTV^{2+} requires a G:H ratio of at least 1:2 to form predominantly the DTV^{2+}@2CB7 complex.

Determination of the Complexation Constant of DTV^{2+}@2CB7 in Water. Changes in the absorption spectra are frequently used to study complexation constants of CBs complexes.[67,68] The complexation constant for the 1:2 complex of DTV^{2+} (the guest, G) with CB7 (the host, H) was determined by monitoring the UV−vis spectral changes at 335 nm (ΔA_{obs} in eq 4 and Figure S9) upon titration of a 5 μM solution of viologen (2 mL) by addition of 5 μL aliquots of a 2 mM aqueous solution of CB7. The data points were plotted against the concentration of CB7 and fitted as shown in Figure 3. For the complexation constant calculations for the 1:2 G:H complex, we employed eqs 2−4, as recently described by Thordarson.[69] This approach involves the formation of a 1:1 complex (eq 2) with complexation constant K_1 followed by association of a second host molecule with the 1:1 complex to form the 1:2 complex (eq 3) with complexation constant K_2.

$$[G] + [H] \rightleftarrows [HG] \qquad K_1 = \frac{[HG]}{[H][G]} \tag{2}$$

$$[HG] + [H] \rightleftarrows [H_2G] \qquad K_2 = \frac{[H_2G]}{[HG][H]} \tag{3}$$

ΔA_{obs}, the absorption change upon titration of DTV^{2+} with CB7, was determined using eq 4:[69]

$$\Delta A_{obs} = \frac{\varepsilon_{\Delta[HG]}[G]_0 K_1[H] + 2\varepsilon_{\Delta[H_2G]}[G]_0 K_1 K_2[H]^2}{1 + K_1[H] + K_1K_2[H]^2} \tag{4}$$

were determined as in Eq.4, where $\varepsilon_{\Delta[HG]}$ and $\varepsilon_{\Delta[H2G]}$ are the extinction coefficients measured at the Host: Guest ratios 1:1 and 2:1, respectively.[69] The complexation constants in water calculated using this method were $K_1 = (1.2 \pm 0.3) \times 10^4\ M^{-1}$ and $K_2 = (1.0 \pm 0.4) \times 10^4\ M^{-1}$. We did not calculate the complexation constant in the presence of excess NaCl because of the complexity of the equilibria involving an additional component and the uncertainty in the number of sodium ions coordinating to the host.

UV−Vis Absorption Spectra and Steady-State and Time-Resolved Fluorescence of DTV^{2+}@2CB7. The absorption (λ_{max} = 335 nm) and emission (λ_{em} = 470 nm) spectra of DTV^{2+}@2CB7 in water exhibited an exceptionally large Stokes shift ($\Delta St \sim 9000\ cm^{-1}$), and no fine structure was present in the room-temperature fluorescence spectrum (Figure 4a).

Aqueous solutions of DTV^{2+} in the absence of the host exhibited a low fluorescence quantum yield (Φ = 0.01), as shown in Table 1 and Figure 4b. Upon addition of CB7 aliquots, however, the emission spectra showed a progressive fluorescence enhancement and a blue shift of the emission band. The emission spectra stabilized at a G:H ratio of about 1:2, at which point further addition of the host did not result in increased emission. Overall, the encapsulation in the host resulted in a 1 order of magnitude enhancement of the emission yield and a blue shift of approximately 35 nm in the maximum (λ_{em} from 505 to 470 nm). Figure 5a shows the titration curves of DTV^{2+} with CB7 in aqueous solution and in the presence of excess NaCl. The integrated emission intensity at each titration step was plotted against the number of equivalents of CB7. The maximum emission intensity was reached at a G:H ratio of 1:2 and is qualitatively consistent with the observations shown in Figure 4b. The stoichiometry of the complex was determined by the continuous variation method[70] (Job plot, shown in Figure 5b) using emission spectroscopy. The total molar concentration of host and guest was held constant at 0.6 mM, and the mole fractions were incrementally varied, while the integrated fluorescence intensity was monitored. The titration plots in Figure 5 suggest that the maximum enhancement was observed for the fully encapsulated DTV^{2+} and that the stoichiometry of the complex is G:H = 1:2, consistent with the ^{1}H NMR spectral changes. Overall, the experiments suggest that in this case the presence of excess NaCl did not result in dramatic changes of the fluorescence or complexation stoichiometry. However, it is widely acknowledged that in studies involving CB hosts, it is preferable to control the concentration of salts, or at least to assess the effect of their presence on the complexation equilibria.[71,72,57,73]

dx.doi.org/10.1021/ja206833z | J. Am. Chem. Soc. 2012, 134, 3358−3366

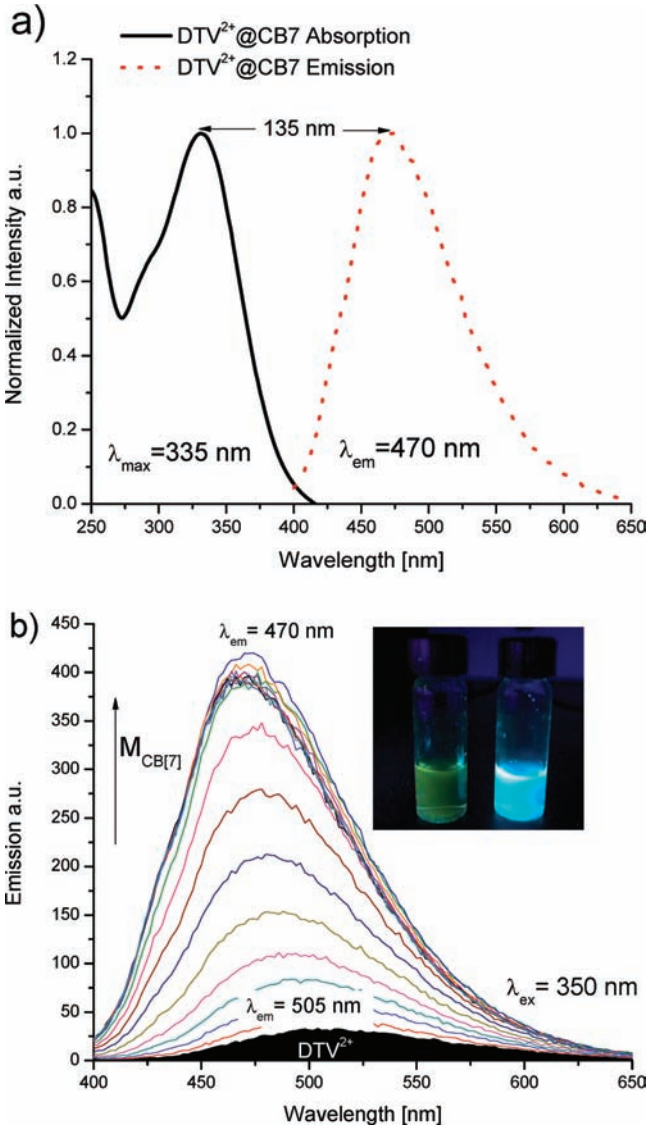

Figure 4. (a) Normalized absorption and emission spectra of DTV^{2+}@2CB7 in aqueous solution. (b) Emission spectra of DTV^{2+} (5 μM) upon addition of CB7 (concentration range: 1−15 μM). λ_{ex} = 350 nm. Inset: Solutions of (left) DTV^{2+} and (right) DTV^{2+}@2CB7 exposed to black light.

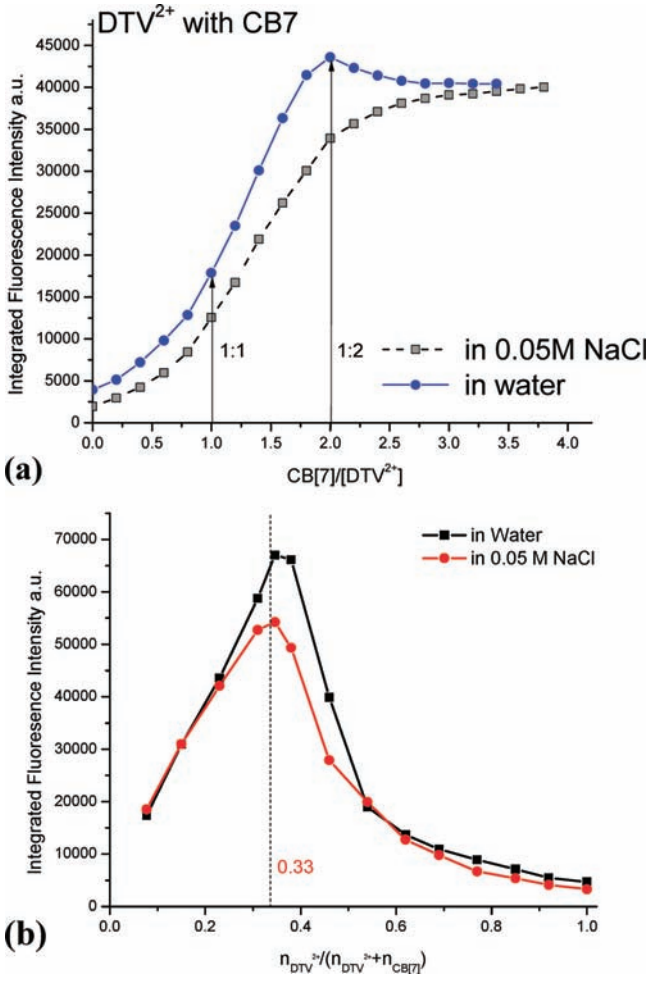

Figure 5. (a) Fluorescence emission titration curve of 5 μM DTV^{2+} with CB7 in water (●, blue line) and in presence of 0.05 M NaCl (■, dashed black line). λ_{ex} = 350 nm. (b) Job plot for the complexation of CB7 in DTV^{2+}. The total concentration [CB7] + [DTV^{2+}] was maintained at 0.6 mM.

Table 1. Selected Photophysical Properties of Aqueous Solutions of DTV^{2+} and its CB7 Complexes

DTV^{2+}:CB7	λ_{em} (nm)	Φ^a	τ (ns)^b
1:0	505	0.01	<0.02 ± 0.004
1:1	482	0.08	0.4 ± 0.08
1:2	470	0.12	0.7 ± 0.14
1:3	470	0.12	0.7 ± 0.14

^{a}Stilbene 420 was used as the reference (see the Experimental Section). λ_{ex} = 320 for the reference and the samples. The uncertainty in the Φ values is ±0.01. $^b\lambda_{ex}$ = 350 nm.

Quantum yields for DTV^{2+} were measured in the presence of 0, 1, 2, and 3 equiv of CB7, in water, as shown in Table 1. The formation of the CB7 complexes resulted in a significant fluorescence quantum yield and lifetime enhancement. The quantum yield of DTV^{2+} was Φ = 0.01, whereas the quantum yield of the CB7 complex increased up to Φ = 0.12, depending on the G:H ratio (Table 1).

The fluorescence lifetime of 2 μM aqueous solutions of DTV^{2+} was <20 ps, which was within the time resolution of the instrument. Bleaching of the DTV^{2+} sample occurred during the measurement, and this was ascribed to sample degradation. This is consistent with the observation that aqueous solutions of samples left in the laboratory environment for prolonged periods of time (weeks) were no longer emissive. Upon addition of 1 and 2 equiv of CB7, the emission lifetime for the complexes was dependent on the DTV^{2+}@CB7 complex stoichiometry and determined to be $\tau_{1:1}$ = 0.4 ns and $\tau_{1:2}$ = 0.7 ns (Figure S10 and Table 1). The increase in fluorescence lifetime is quantitatively consistent with the increase in emission intensity. The time-resolved experiments were repeated in the presence of a large excess of NaCl (0.05 M), and the results were, within the experimental error, identical to what was observed in water.

To explore the influence of conformation restrictions of DTV^{2+} on the emission properties, DTV^{2+} was mixed with PMMA polymer and spin-coated into films. The emission spectra of DTV^{2+} in a PMMA matrix (Figure 6) showed a blue-shifted, structureless emission band (λ_{em} = 465 nm) similar to that observed upon encapsulation into CB7.

dx.doi.org/10.1021/ja206833z | J. Am. Chem. Soc. 2012, 134, 3358−3366

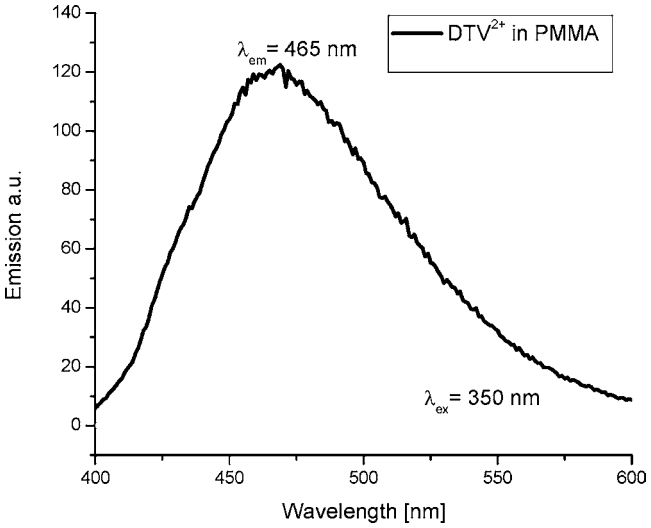

Figure 6. Emission spectrum of DTV^{2+} (8.0 wt %) in a PMMA polymer matrix.

DFT and CIS Calculations. DFT and CIS calculations showed that the formation of the S_1 state and the subsequent intersystem crossing to the T_1 state are associated with major changes of the dihedral angles between the four aromatic rings of the DTV^{2+} molecule, as shown in Figure 7, top. Such large-

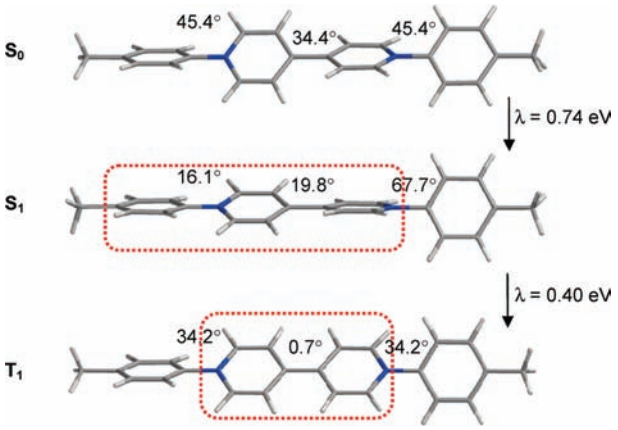

Figure 7. Optimized structures of the S_0, S_1, and T_1 states of DTV^{2+}, indicating the inter-ring dihedral angles as well as the $\lambda(S_0-S_1)$ and $\lambda(S_1-T_1)$ intramolecular reorganization energies. The dashed boxes indicate the almost planar geometries of three consecutive rings in the S_1 state and the two bipyridyl rings in the T_1 state.

amplitude relaxation processes are certainly hindered and considerably slowed in a PMMA matrix as well as upon encapsulation in the CB7 host. The ground-state equilibrium conformation of DTV^{2+}, with a 34.4° dihedral angle of the viologen core, is close to the 35° dihedral angle for the ground state of the isoelectronic biphenyl. In the relaxed S_1 state, the twofold symmetry of the system is broken, reflecting the intermolecular charge-transfer nature of the transition. The viologen core and one of the *p*-tolyl moieties are more planar and form a strongly coupled sequence of three rings, while the fourth *p*-tolyl moiety is twisted (65.5°) with respect to the rest of the molecule (Figure 7). The respective dihedral angle changes in the $S_0 \rightarrow S_1$ transition are shown in Figure 7.

The planarized section of the ring sequence in the S_1 state adopts a pronounced quinonoid structure as illustrated in Figure 8. Most notably, the length of bond "d" connecting the nearly coplanar *p*-tolyl moiety to the viologen core decreases

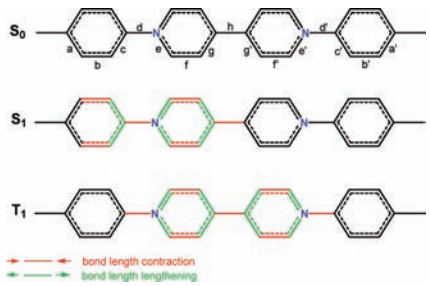

Figure 8. Illustration of the bond lengths in the S_1 state of DTV^{2+}. The last *p*-tolyl ring's bond lengths are all identical. Bonds whose lengths change by more than 0.025 Å compared with those in the S_0 state are shown in color (contraction in red and lengthening in green), and bonds in black are all identical in length. A similar illustration for the T_1 state is also shown. For bond lengths, see Table 2.

from 1.45 Å to a double-bond-like 1.34 Å. The complete set of calculated bond lengths in the S_0, S_1, and T_1 states is given in Table 2.

The formation of the T_1 state is associated with another large geometry change. In this case, the viologen core adopts a completely planar quinonoid structure, while both *p*-tolyl groups are rotated out-of-plane considerably. The large geometry changes associated with the $S_0 \rightarrow S_1$ and $S_1 \rightarrow T_1$ transitions are accompanied by large intramolecular reorganization energies [$\lambda(S_0-S_1)$ = 0.74 eV and $\lambda(S_1-T_1)$ = 0.40 eV, respectively]. The particularly large value of $\lambda(S_0-S_1)$ explains the lack of vibronic structure in the absorption and emission spectra of DTV^{2+}.

Consistent with the experimental observations of the changes in the emission spectra of DTV^{2+} in solution and in a confining medium (PMMA or a host), the calculations predicted a 0.74 eV red shift of the S_1-S_0 transition upon relaxation from the Franck–Condon state to the optimum S_1 geometry. The blue shift of the emission maximum is therefore the result of going from a fluid to a confining medium, which prevents such relaxation.[74] The blue shift could also be explained by the different polarities experienced by DTV^{2+} in CB7 and in water.

Furthermore, the calculations revealed that the oscillator strength of the $S_1 \rightarrow S_0$ transition diminishes from 0.79 in the geometry of the ground state to 0.20 in the relaxed geometry of the S_1 state. This 4-fold reduction cannot fully account for the essentially complete quenching of the fluorescence of DTV^{2+} in water. An oscillator strength of 0.2 in the fully relaxed geometry would lead to substantial emission unless the system undergoes further nonradiative decay. We postulate that the low emission quantum yield and the very short (<20 ps) excited-state lifetime can be ascribed to rapid intersystem crossing and internal conversion occurring on a time scale that is similar to or only slightly longer than the S_1 relaxation. Any hindrance or retardation of the rotation of the four rings of DTV^{2+}, as for instance by a polymer matrix or confinement in a host, would slow the intersystem crossing and internal conversion and result in lengthening of the S_1 lifetime and increased fluorescence quantum yield, as observed in the reported experiments. The 4-fold reduction in the oscillator strength does not fully account for the experimentally observed fluorescence quantum yields of the free and encapsulated DTV^{2+}, which differ by a factor of nearly 15. Clearly, DTV^{2+} in

dx.doi.org/10.1021/ja206833z | J. Am. Chem. Soc. 2012, 134, 3358–3366

Table 2. Calculated C−C and C−N Bond Lengths of the Conjugated Core of DTV^{2+} in the S_0, S_1, and T_1 Electronic States[a]

	a	b	c	d	e	f	g	h	g′	f′	e′	d′	c′	b′	a′
S_0	1.41	1.39	1.40	1.45	1.36	1.38	1.41	1.48	1.41	1.38	1.36	1.45	1.40	1.39	1.41
S_1	1.42	1.36	1.44	1.34	1.42	1.34	1.43	1.45	1.41	1.37	1.34	1.46	1.39	1.38	1.40
T_1	1.42	1.38	1.42	1.42	1.39	1.36	1.44	1.42	1.44	1.36	1.39	1.42	1.41	1.38	1.42

[a]All values in Å. See Figure 8 for labeling of the bonds.

aqueous solution is subject to additional nonradiative deactivation processes, such as a rearrangement of the solvation shell, which are also hindered upon encapsulation. The chloride counterion is more tightly associated to DTV^{2+} in aqueous solutions than in the complex[46] and could also play a role in modulating the emission yield. For this reason, it could be interesting to study the effect of softer counterions.

In conclusion, the excited-state rotational dynamics of the DTV^{2+} guest appears to play the key role in the observed enhancement and blue shift of the emission and is augmented by solvation and ion-association effects. Precedent for this effect can be found in the study by Bhasikuttan, Nau, and co-workers of the dye Brilliant Green, a triphenylmethane derivative, where restriction of intramolecular bond rotations between the aryl rings induced by complexation with CB7 and a protein resulted in enhanced fluorescence.[75]

Electrochemistry. The one-electron reduction process of viologens (Scheme 2) is fast and reversible, and the radical cation is intensely blue colored.[1,76] DTV^{2+} showed the same reversibility and a more positive reduction potential, indicating that DTV^{2+} is a better electron acceptor than methyl viologen (Figure S6 and Table 3). It should be noted, however, that the current−potential curves are distorted from fully reversible shapes, probably because of partial precipitation of the reduced form on the electrode surface. The shift to a more negative potential in the cyclic voltammogram of DTV^{2+} upon encapsulation in CB7 (Figure S6), although very small and possibly close to an experimental error, is consistent with similar observations for other viologens[35,34] and can be ascribed to a decreased affinity of the radical cation for CB7 relative to that of the dication.[34]

Scheme 2. One-Electron Reduction of MV^{2+} (R = Me) and DTV^{2+} (R = *p*-Tolyl)

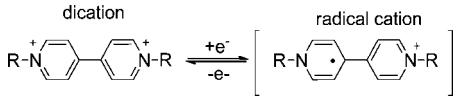

Table 3. Voltammetric Parameters for Free and Encapsulated MV^{2+} and DTV^{2+}

compound	$E^0_{1/2}$ (V)[b]
MV^{2+}[a]	−0.66
MV^{2+}@CB7[a]	−0.68
DTV^{2+}	−0.35
DTV^{2+}@2CB7	−0.36

[a]Data from ref 35. The experiments from the literature were conducted in aqueous 0.1 M phosphate buffer (pH 7.3) using an Ag/AgCl (3.0 M NaCl) electrode. [b]Half-wave potentials for the first reduction process vs saturated Ag/AgCl (3.0 M NaCl) reference electrode in 0.1 M aqueous phosphate buffer (pH 7.3).

The absorption and fluorescence spectra of the $DTV^{\bullet+}$@2CB7 complex are shown in Figure 9 a,b, and those for the free radical cation $DTV^{\bullet+}$ are shown in Figures S7 and S8. The absorption spectrum of $DTV^{\bullet+}$@2CB7 is identical to the spectrum of free $DTV^{\bullet+}$ and considerably blue-shifted (λ_{max} = 400 nm) relative to the spectra of the free methyl viologen radical cation and of $MV^{\bullet+}$complexed in CB7 (λ_{max} = 600 nm). The fluorescence spectra of the one-electron-reduced complex $DTV^{\bullet+}$@2CB7 (Figure 9b) and of free $DTV^{\bullet+}$ (Figure S8) indicate that $DTV^{\bullet+}$ is not emissive.

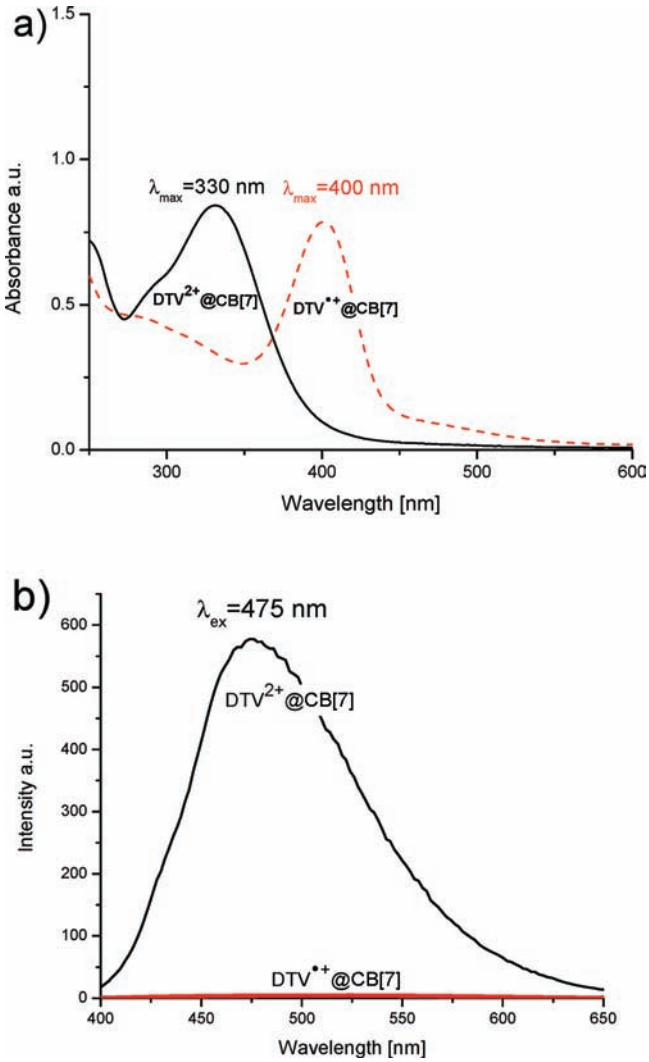

Figure 9. (a) Absorption and (b) emission spectra of DTV^{2+}@2CB7 in water before (black solid line) and after (red dashed line) one-electron reduction to the radical cation $DTV^{\bullet+}$@2CB7 by application of −1.0 V. λ_{exc} = 350 nm.

Finally, DTV^{2+}@2CB7 is a strong photooxidant. The singlet-excited-state reduction potential, $E^\circ(DTV^{2+*}/DTV^{\bullet+})$, was

dx.doi.org/10.1021/ja206833z | J. Am. Chem. Soc. 2012, 134, 3358−3366

estimated to be +2.93 eV vs NHE on the basis of the singlet energy, E_{00} = 3.09 eV, and the ground-state reduction potential, $E°(DTV^{2+}@2CB7/DTV^{\bullet+}@2CB7)$ = −0.156 V vs NHE. This is consistent with the singlet-excited-state reduction potential for methyl viologen reported by Kohler,[46] which was estimated to be +3.65 eV vs NHE.

CONCLUSIONS

We have presented the first example of fluorescence enhancement of *p*-tolyl viologen, DTV^{2+}, upon encapsulation in CB7 in aqueous solutions or casting in PMMA films. The encapsulation process and the stoichiometry of the complex were determined by ^{1}H NMR spectroscopy and Job plot analysis. The ^{1}H NMR spectra in aqueous solutions and in the presence of excess NaCl indicated that DTV^{2+} forms a 1:2 G:H complex with CB7. Smaller H:G ratios resulted in broadening of the NMR spectra, suggesting a dynamic distribution of species during the time scale of the NMR experiment.

The $DTV^{2+}@2CB7$ complexes exhibited a fluorescence enhancement of about 1 order of magnitude relative to free DTV^{2+}. Simultaneously, the emission lifetime increased from <20 ps to 0.7 ns. A blue shift of ∼35 nm was observed upon addition of increasing amounts of CB7 host (from 0 to 2 equiv) to DTV^{2+}. The presence of NaCl or oxygen did not significantly change the emissive behavior of the complex. The fluorescence emission of DTV^{2+} and the blue shift were also observed in PMMA films.

Such enhancement had not been observed for alkyl or phenyl viologen complexes of CB7, suggesting that the structure of the quaternizing moieties, in this case the *p*-tolyl units, is important. DFT and CIS calculations predicted that the relaxed S_1 state has a strongly coupled sequence of three nearly coplanar rings (one *p*-tolyl ring and the two rings of the 4,4′-bipyridium core) exhibiting a quinonoid structure with alternating bond lengths. Encapsulation in the host or casting in a film prevents the system from adopting this geometry and results in dramatically increased emission.

DTV^{2+} is a strong photooxidant and a good electron acceptor. The electrochemical one-electron reductions of $DTV^{2+}$and $DTV^{2+}@2CB7$ to $DTV^{\bullet+}$ and $DTV^{\bullet+}@2CB7$, respectively, were reversible. The absorption and emission properties of the radical cations suggest that DTV^{2+} and $DTV^{2+}@n$CB7 could be useful in the development of electrochomic materials and fluorescence switches.

In conclusion, this work suggests that the methyl group on the *p*-tolyl moiety of a viologen, combined with conformational constraints induced by a host, results in a dramatic fluorescence enhancement. This concept will be further expanded to tune the emissive and electrochemical properties of similar viologen derivatives encapsulated and bound to semiconductor layers, following the procedures developed for DTV^{2+} and MV^{2+}; however, the poor solubility of CB7 complexes is a limitation.[35] The electrochemical properties suggest that DTV^{2+} derivatives might find applications in electrochromic windows, as substituents on the tolyl groups may result in color tuning, and the ability to switch the fluorescence of the $DTV^{2+}@CB7$ complexes on and off electrochemically is potentially attractive for LED applications. Studies of the properties of the complexes on metal oxide semiconductor interfaces and the effect of softer counterions on the photophysical properties of DTV^{2+} in solution are in progress.

ASSOCIATED CONTENT

Supporting Information

Synthesis and characterization of **1**, ^{1}H NMR spectra of CB7 and DTV^{2+}, UV−vis spectra for the determination of binding constants, ^{1}H NMR spectra of the CB7 region, absorption and emission spectra of $DTV^{\bullet+}$, cyclic voltammograms of DTV^{2+} and $DTV^{2+}@2CB7$, and experimental procedure for the Job plot. This material is available free of charge via the Internet at http://pubs.acs.org.

AUTHOR INFORMATION

Corresponding Author

galoppin@rutgers.edu

Present Address

[†]Department of Chemistry and Biochemistry, University of Delaware, Newark, DE 19716.

ACKNOWLEDGMENTS

E.G. thanks Prof. Cornelia Bohne for a discussion of the role of NaCl in CB7 complexation processes and Ms. Yan Cao for quantum yield measurements with Stilbene 420. The authors thank the American Chemical Society Petroleum Research Fund (Grant 46663-AC10) for support. The FT-IR-ATR spectra, time-resolved measurements, and DFT calculations were made possible by funding by the Office of Basic Energy Sciences of the U.S. Department of Energy through Grant DE-FG02-01ER15256. P.P. thanks NSFR Grant # 0923345 for support.

REFERENCES

(1) Monk, P. M. S. *The Viologens: Physicochemical Properties, Synthesis and Applications of the Salts of 4,4′-Bipyridine*; Wiley: New York, 1998.
(2) Cinnsealach, R.; Boschloo, G.; Rao, S. N.; Fitzmaurice, D. *Sol. Energy Mater. Sol. Cells* **1998**, *55*, 215−218.
(3) Campus, F.; Bonhote, P.; Grätzel, M.; Heinen, S.; Walder, L. *Sol. Energy Mater. Sol. Cells* **1999**, *56*, 281−297.
(4) Cummins, D.; Boschloo, G.; Ryan, M.; Corr, D.; Rao, S. N.; Fitzmaurice, D. *J. Phys. Chem. B* **2000**, *104*, 11449−11459.
(5) Lee, J. W.; Samal, S.; Selvapalam, N.; Kim, H. J.; Kim, K. *Acc. Chem. Res.* **2003**, *36*, 621−630.
(6) Flood, A. H.; Stoddart, J. F.; Steuerman, D. W.; Heath, J. R. *Science* **2004**, *306*, 2055−2061.
(7) Luo, Y.; Collier, C. P.; Jeppesen, J. O.; Nielsen, K. A.; DeIonno, E.; Ho, G.; Perkins, J.; Tseng, H.-R.; Yamamoto, T.; Stoddart, J. F.; Heath, J. R. *ChemPhysChem* **2002**, *3*, 519−525.
(8) Smith, E. A.; Lilienthal, R. R.; Fonseca, R. J.; Smith, D. K. *Anal. Chem.* **1994**, *66*, 3013−3020.
(9) Kaifer, A. E. *Acc. Chem. Res.* **1999**, *32*, 62−71.
(10) Pía, E.; Toba, R.; Chas, M.; Peinador, C.; Quintela, J. M. *Tetrahedron Lett.* **2006**, *47*, 1953−1956.
(11) Ploug-Sørensen, A.; Nielsen, M. B.; Becher, J. *Tetrahedron Lett.* **2003**, *44*, 2979−2982.
(12) Benniston, A. C. *Chem. Soc. Rev.* **2004**, *33*, 573−578.
(13) Ramaiah, D.; Neelakandan, P. P.; Nair, A. K.; Avirah, R. R. *Chem. Soc. Rev.* **2010**, *39*, 4158−4168.
(14) Park, J. W.; Song, H. J.; Chang, H.-J. *Tetrahedron Lett.* **2006**, *47*, 3831−3834.
(15) Long, B.; Nikitin, K.; Fitzmaurice, D. *J. Am. Chem. Soc.* **2003**, *125*, 15490−15498.
(16) Qu, D.-H.; Tian, H. *Chem. Sci.* **2011**, *2*, 1011−1015.
(17) Nepogodiev, S. A.; Stoddart, J. F. *Chem. Rev.* **1998**, *98*, 1959−1976.
(18) Trabolsi, A.; Khashab, N.; Fahrenbach, A. C.; Friedman, D. C.; Colvin, M. T.; Cotí, K. K.; Benítez, D.; Tkatchouz, E.; Olsen, J.-C.;

Belowich, M. E.; Carmielli, R.; Khatib, H. A.; Goddard, W. A. III; Wasielewski, M. R.; Stoddart, J. F. *Nat. Chem.* **2010**, *2*, 42−49.
(19) Coronado, E.; Gavin, P.; Tatay, S. *Chem. Soc. Rev.* **2009**, *38*, 1674−1689.
(20) Holmlin, R. E.; Dandliker, P. J.; Barton, J. K. *Angew. Chem., Int. Ed. Engl.* **1997**, *36*, 2714−2730.
(21) Balzani, V. *Electron Transfer in Chemistry*; Wiley-VCH: Weinheim, Germany, 2008.
(22) Yonemoto, E. H.; Saupe, G. B.; Schmehl, R. H.; Stefan, S.; Hubig, M.; Riley, R. L.; Iverson, B. L.; Mallouk, T. E. *J. Am. Chem. Soc.* **1994**, *116*, 4786−4795.
(23) Nelissen, H. F. M.; Kercher, M.; De Cola, L.; Feiters, M. C. R.; Nolte, J. M. *Chem.—Eur. J.* **2002**, *8*, 5407−5414.
(24) Esswein, A. J.; Nocera, D. G. *Chem. Rev.* **2007**, *107*, 4022−4047.
(25) Youngblood, W. J.; Lee, S.-H. A.; Maeda, K.; Mallouk, T. E. *Acc. Chem. Res.* **2009**, *42*, 1966−1973.
(26) Clennan, E. L. *Coord. Chem. Rev.* **2004**, *248*, 477−492.
(27) Da Silva, S.; Cosnier, S.; Almeida, M. G.; Moura, J. J. G. *Electrochem. Commun.* **2004**, *6*, 404−408.
(28) Liu, X.; Neoh, K. G.; Cen, L.; Kang, E. T. *Biosens. Bioelectron.* **2004**, *19*, 823−834.
(29) Steed, J. W.; Atwood, J. L. *Supramolecular Chemistry*, 2nd ed.; Wiley: Chichester, U.K., 2009.
(30) Kim, K.; Selvapalam, N.; Oh, D. H. *J. Inclusion Phenom. Macrocyclic Chem.* **2004**, *50*, 31−36.
(31) Lagona, J.; Mukhopadhyay, P.; Chakrabarti, S.; Isaacs, L. *Angew. Chem., Int. Ed.* **2005**, *44*, 4844−4870.
(32) Sindelar, V.; Silvi, S.; Kaifer, A. E. *Chem. Commun.* **2006**, 2185−2187.
(33) Kim, H. J.; Jeon, W. S.; Ko, Y. H.; Kim, K. *Proc. Natl. Acad. Sci. U.S.A.* **2002**, *99*, 5007−5011.
(34) Kim, K.; Selvapalam, N.; Ko, Y. H.; Park, K. M.; Kim, D.; Kim, K. J. *Chem. Soc. Rev.* **2007**, *36*, 267−279.
(35) Freitag, M.; Galoppini, E. *Langmuir* **2010**, *26*, 8262−8269.
(36) Kavarnos, G. J.; Turro, N. J. *Chem. Rev.* **1986**, *86*, 401−449.
(37) Haeupl, T.; Lomoth, R.; Hammarström, L. *J. Phys. Chem. A* **2003**, *107*, 435−438.
(38) Clark, C. D.; Debad, J. D.; Yonemoto, E. H.; Mallouk, T. E.; Bard, A. J. *J. Am. Chem. Soc.* **1997**, *119*, 10525−10531.
(39) Alvaro, M.; Garcia, H.; Garcia, S.; Marquez, F.; Scaiano, J. C. *J. Phys. Chem. B* **1997**, *101*, 3043−3051.
(40) Barnett, J. R.; Hopkins, A. S.; Ledwith, A. *J. Chem. Soc., Perkin Trans. 2* **1973**, 80−84.
(41) Ebbesen, T. W.; Manring, L. E.; Peters, K. S. *J. Am. Chem. Soc.* **1984**, *106*, 7400−7404.
(42) Novakovic, V.; Hoffman, M. Z. *J. Am. Chem. Soc.* **1987**, *109*, 2341−2346.
(43) Such impurities can be formed during the synthesis or by long exposure to light and air, as mentioned by refs 45 and 1.
(44) Alvaro, M.; Facey, G. A.; García, H.; García, S.; Scaiano, J. C. *J. Phys. Chem.* **1996**, *100*, 18173−18176.
(45) Mau, A. W.-H.; Overbeek, J. M.; Loder, J. W.; Sasse, W. H. F. *J. Chem. Soc., Faraday Trans. 2* **1986**, *82*, 869−876.
(46) Peon, J.; Tan, X.; Hoerner, J. D.; Xia, C.; Luk, Y. F.; Kohler, B. *J. Phys. Chem. A* **2001**, *105*, 5768−5777.
(47) Marquez, C.; Huang, F.; Nau, W. M. *IEEE Trans. Nanobiosci.* **2004**, *3*, 39−45.
(48) Koner, A. L.; Nau, W. M. *Supramol. Chem.* **2007**, *19*, 55−66.
(49) Parvari, G.; Reany, O.; Keinan, E. *Isr. J. Chem.* **2011**, *51*, 646−663.
(50) Metrangolo, P.; Resnati, G. In *Encyclopedia of Supramolecular Chemistry*; Atwood, J. L., Steed, J. W., Eds.; Marcel Dekker: New York, 2004.
(51) Wang, R.; Yuan, L.; Macartney, D. H. *J. Org. Chem.* **2006**, *71*, 1237−1239.
(52) Freitag, M.; Galoppini, E. *Energy Environ. Sci.* **2011**, *4*, 2482−2494.
(53) Maddlipata, M. V. S. N.; Kaanumalle, L. S.; Natarajan, A.; Pattabiraman, M.; Ramamurthy, V. *Langmuir* **2007**, *23*, 7545−7554.
(54) Marquez, C.; Hudgins, R. R.; Nau, W. M. *J. Am. Chem. Soc.* **2004**, *126*, 5806−5816.
(55) Megyesi, M.; Biczók, L.; Jablonkai, I. *J. Phys. Chem. C* **2008**, *112*, 3410−3416.
(56) Shaikh, M.; Mohanty, J.; Bhasikuttan, A. C.; Uzunova, V. D.; Nau, W. M.; Pal, H. *Chem. Commun.* **2008**, 3681−3683.
(57) Rekharsky, M. V.; Inoue, Y. *Netsu Sokutei* **2007**, *34*, 232−243.
(58) Khan, M. S. A.; Heger, D.; Necas, M.; Sindelar, V. *J. Phys. Chem. B* **2009**, *113*, 11055−11061.
(59) Bos, F. *Appl. Opt.* **1981**, *20*, 3553−3556.
(60) Gundlach, L.; Piotrowiak, P. *Opt. Lett.* **2008**, *33*, 992−994.
(61) Kamogawa, H.; Satoh, S. *J. Polym. Sci., Part A: Polym. Chem.* **1988**, *26*, 653−656.
(62) Zincke, T. H.; Weisspfenning, G. *Justus Liebigs Ann. Chem.* **1913**, *396*, 103−131.
(63) Kunugi, S.; Okubo, T.; Ise, N. *J. Am. Chem. Soc.* **1976**, *98*, 2282−2287.
(64) Montes-Navajas, P.; Corma, A.; Garcia, H. *J. Mol. Catal. A: Chem.* **2008**, *279*, 165−169.
(65) Moon, K.; Kaifer, A. E. *Org. Lett.* **2004**, *6*, 185−188.
(66) Wang, R.; Bardelang, D.; Waite, M.; Udachin, K. A.; Leek, D. M.; Yu, K.; Ratcliffe, C. I.; Ripmeester, J. A. *Org. Biomol. Chem.* **2009**, *7*, 2435−2439.
(67) Ong, W.; Kaifer, A. E. *Angew. Chem., Int. Ed.* **2003**, *42*, 2164−2167.
(68) Ong, W.; Comez-Kaifer, M.; Kaifer, A. E. *Org. Lett.* **2002**, *4*, 1791−1794.
(69) Thordarson, P. *Chem. Soc. Rev.* **2011**, *40*, 1305−1323. We used the equations in Chart 3 on p 1311.
(70) Connors, K. A. *Binding Constants*; Wiley: New York, 1987; Chapter 4.
(71) Kaifer, A. E.; Li, W.; Yi, S. *Isr. J. Chem.* **2011**, *51*, 496−505.
(72) Ong, W.; Kaifer, A. E. *J. Org. Chem.* **2004**, *69*, 1383−1385.
(73) Tang, H.; Fuentealba, D.; Ko, Y. H.; Narayanan, S.; Kim, K.; Bohne, C. *J. Am. Chem. Soc.* **2011**, *133*, 20623−20633.
(74) Barigelletti, F.; Belser, P.; von Zelewsky, A.; Juris, A.; Balzani, V. *J. Phys. Chem.* **1985**, *89*, 3680−3684.
(75) Bhasikuttan, A. C.; Mohanty, J.; Nau, W. M.; Pal, H. *Angew. Chem., Int. Ed.* **2007**, *46*, 4120−4122.
(76) Mortimer, R. J.; Reynolds, J. R. *Displays* **2008**, *29*, 424−431.